Trajectory initialization and calibration using a foot-mounted IMU and UWB anchors

Yang Gu, Ming Ma, Qian Song, Zhimin Zhou
College of Electronic Science
National University of Defense Technology
Changsha, Hunan, China
guyang@nudt.edu.cn, maming09@126.com, songqian@nudt.edu.cn, kdzhouzm@sina.cn

***Abstract*—Inertial based pedestrian positioning is very useful in emergency response situations, such as search and rescue (SAR) missions as it is independent of external infrastructures and signals. Two practical problems emerge in inertial based pedestrian positioning: trajectory initialization and trajectory calibration. The former one denotes how to determine the initial position and heading of the pedestrian, and the latter denotes how to reduce the dead reckoning (DR) errors due to inertial drifts. This paper provides a solution to these two problems adopting a few ultra-wide band (UWB) anchors, which can provide range measurements between the anchors and the pedestrian. The foundation of the method is graph based simultaneously localization and mapping (SLAM). The nodes in the graph are the poses of the pedestrian and the edges are the range measurements between the UWB anchors and the tags mounted on the pedestrian. Both simulations and real scenario experiments are carried out to validate the proposed method. The proposed approach outperformed the particle filtering based approach in terms of robustness and processing time.**

Keywords-*indoor positioning; UWB ranging; foot-mounted IMU; graph based SLAM*

I. INTRODUCTION

With a miniaturized micro-electro-mechanical system (MEMS) inertial measurement unit (IMU) mounted on the foot, a pedestrian's positions can be tracked [1] [2] . As an IMU is self-contained and independent of external infrastructures and signals, this foot-mounted indoor positioning (FMIP) is useful in emergency response situations such as search and rescue (SAR) missions. However, there are still two problems which hinders the application of FMIP: trajectory initialization and trajectory calibration.

A initial position and heading should be known prior to dead reckoning (DR) with FMIP. Sometimes default initial states can be assumed, however, problems will emerge when multiple agents are tracked. As the actual initial states of agents may be different, an unified initial state assumption can damage the physical geometric relations between agents. To obtain the users' trajectories in an unified well defined coordinate system, the trajectory initialization problem should be solved. Trajectory calibration denotes reducing the positioning errors due to inertial drifts. Although the inertial drifts are already significantly suppressed by adopting the motion model of the user's foot using the zero-velocity update (ZUPT) algorithm [3] [4], the positioning errors in a long term still needs calibration.

978-1-5386-3755-5/18/$31.00 © 2018 IEEE

To solve the aforementioned problems, pre-deployed ultra-wide band (UWB) anchors are introduced, which can provide additional range measurements to aid positioning. The anchors can emit Impulse Radio Ultra-WideBand (IR-UWB) signals, which has good ranging performances, such as high resolution, resistance to multi-path, wall-penetration capacity [5] , etc..

The research of dead reckoning and UWB ranging fusion have expanded from robotics [6] [7] to indoor pedestrian positioning in recent years. The authors in [8] pre-installed wireless sensor network (WSN) UWB nodes and utilized the dead-reckoning to help positioning in the UWB signal blind spots. In [9], the raw measurements from inertial sensors and multiple UWB ranging are tightly coupled in an extended Kalman filter (EKF). A cooperative scheme is proposed in [10], which fuses the inertial dead reckoning positions and the inter-agent UWB ranging measurements using a Kalman typed filter. These approaches have various drawbacks. Tight coupling is too computational difficult in real-time considering the high dimension of state filtering, if the global estimation for multi-agents is needed [10]. EKF can not deal with the situation of unknown initial state. Although in [11] a particle filter (PF) is adopted instead of EKF to enable state initialization, the positioning suffers from a failure rate and is greatly affected by the number of particles.

Instead of using a filtering framework, this paper propose to do the fusion using graph based SLAM [12]. Unlike the filtering framework, where only a couple of recent or future measurements (often denoted as smoothing if future measurements are adopted) are adopted to estimate the current state, our method use all available measurements for state estimation to increase robustness and accuracy. Here the poses are the nodes in the graph and the range measurements are the edges. Both simulations and real scenario experiments are carried out to validate the proposed method. According to the comparison with the particle filtering approach, our method is more robust and have less computational cost.

The structure for the remaining paper is as follows. Section II gives an overview for graph based SLAM and the filtering based fusion approaches. Section III is the description of the proposed method in detail. Section IV is the simulations and the experiments for the proposed method and section V is the

conclusion.

II. Background

There are two types of approaches for estimating states in time series: filter based approaches and batch based approaches. Filter based approaches are often in the "predict-update" manner. The posterior distribution of the current state is recursively estimated as new observations become available. However, for such estimation, only a few observations in time is adopted, e.g., nearest one in time, a few nearest ones in the past and a few nearest ones in the past and future (smoothing). Many of the fusion methods for DR and UWB ranging measurements are filter based. Batch based approaches are different, a series of states in time is estimated in a batch adopting all past observations. Graph based SLAM [12] is one of such approaches. Although the computational cost may increase accordingly, the estimation is more accurate and more robust to outliers.

Here a brief introduction of graph based SLAM is given. The states to be estimated and measurements are considered elements in a graph. Specifically, the poses are considered as nodes in the graph and the measurements are considered as edges which represent constraints between the poses. Herein the constraints is comprised of two types: IMU derived constrains and UWB anchor derived constraints. After the graph is constructed, an optimization process for the graph can be carried out, which is is essentially finding the configuration of nodes which satisfies the measurements best. The graph optimization problem is often transformed to minimizing an error function and can be treated as a Least Squares Optimization (LSO) problem. Algorithms like Gauss-Newton or Levenberg-Marquardt [13] can be adopted to solve such problems. In this paper, the general graph optimization (g2o) [14] library is adopted for optimization, which uses a package of algorithms to lower computational cost.

III. Method

Our method has briefly two processes: graph formation and graph optimization, which are also denoted as front-end and back-end. As there are already mature library for graph optimization, we mainly discuss the graph formation process here. The fundamental elements in the graph are firstly introduced and then description of how to adopt the elements to form the overall graph is given. Fig. 1 shows the fundamental elements in the graph: nodes, IMU based edges and UWB based edges.

A. Fundamental elements in the graph

1) Nodes: The nodes are the poses of the pedestrian in equation 1,

$$\mathbf{pos}_i = (x_i, y_i, \theta_i) \tag{1}$$

where the subindex denotes the i_{th} step of the pedestrian, x and y are the horizontal position, θ is the heading. These poses are the states to be estimated through graph optimization. In our implementation, an initial guess is given to the nodes, which is directly taken from the results of inertial calculation

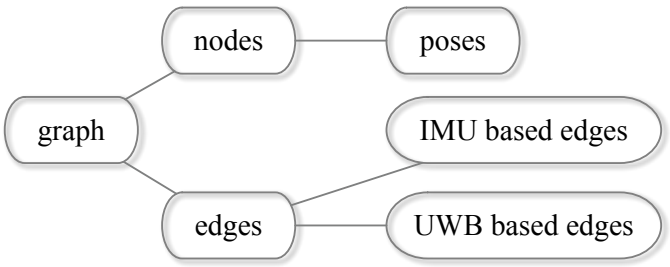

Fig. 1. Elements in the graph

from the output of the foot-mounted IMU. For easy implementation, the starting pose of the DR result is set to

$$\mathbf{pos}_1^i = (0, 0, 0) \tag{2}$$

2) IMU based edges: Between consecutive poses $\mathbf{pos}_{k-1}$ and $\mathbf{pos}_k$ in time, we can calculate a vector $\mathbf{u}_{k-1,k}$ which describes the difference of the two poses as

$$\begin{aligned} \mathbf{u}_{k-1,k} &= \begin{pmatrix} x_k \\ y_k \\ \theta_k \end{pmatrix} - \begin{pmatrix} x_{k-1} \\ y_{k-1} \\ \theta_{k-1} \end{pmatrix} \\ &= \begin{pmatrix} \Delta x_{k-1} cos(\theta_{k-1}) - \Delta y_{k-1} sin(\theta_{k-1}) \\ \Delta x_{k-1} sin(\theta_{k-1}) + \Delta y_{k-1} cos(\theta_{k-1}) \\ \Delta\theta_{k-1} \end{pmatrix} \end{aligned} \tag{3}$$

$\mathbf{u}_{k-1,k}^{\text{estimate}}$, as an estimation of $\mathbf{u}_{k-1,k}$ can also be acquired through the inertial calculation of the IMU. In our implementation, we do not go into details of how the inertial data of the foot-mounted IMU is processed, instead we only consider the IMU as a black box to provide the step-wise DR data (the positions are updated at each step). The constraints to the $k-1^{th}$ and the k^{th} node is essentially a part of the overall error function. As for this constraint, it is

$$f_{\text{IMU}}(k-1,k) = \mathbf{e}_{\text{IMU}}(k-1,k)^{\text{T}} \mathbf{\Omega}_{\text{IMU}} \mathbf{e}_{\text{IMU}}(k-1,k) \tag{4}$$

where

$$\mathbf{e}_{\text{IMU}}(k-1,k) = \mathbf{u}_{k-1,k}^{\text{estimate}} - \mathbf{u}_{k-1,k} \tag{5}$$

and $\mathbf{\Omega}_{\text{IMU}}$ is a 3×3 diagonal information matrix. The information matrix denotes the quality of the measurements. Normally, as the position related error is less trustable than the heading related ones, the position related elements are set much smaller than the heading related ones.

3) UWB based edges: Different from the IMU based edges, the UWB based edges is the constraint between the UWB anchor and the corresponding node, where the ranging measurement is available. In our implementation, the positions of the anchors are already known, so the UWB based edges are unary edges, which only constrain one node for each observation. In the indoor environment, as there are many none-line of sight (NLoS) situations, it is more often that the measured range is larger than the ground truth. Even the NLoS caused by the obstruction of the pedestrian's body from the UWB tag to anchor can add extra range measurement error.

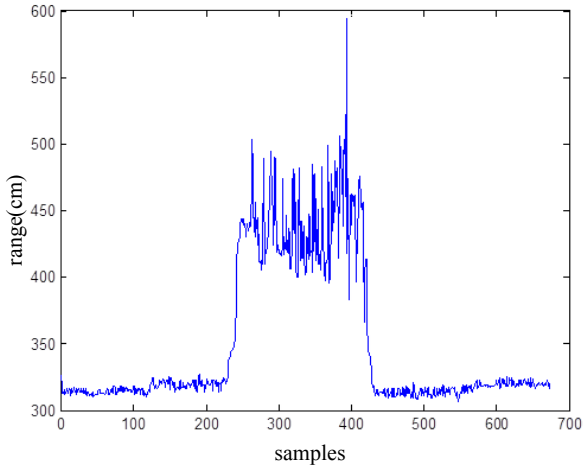

Fig. 2. The range measurement samples when a pedestrian walks around the UWB tag. The real distance is 3.2 meters.

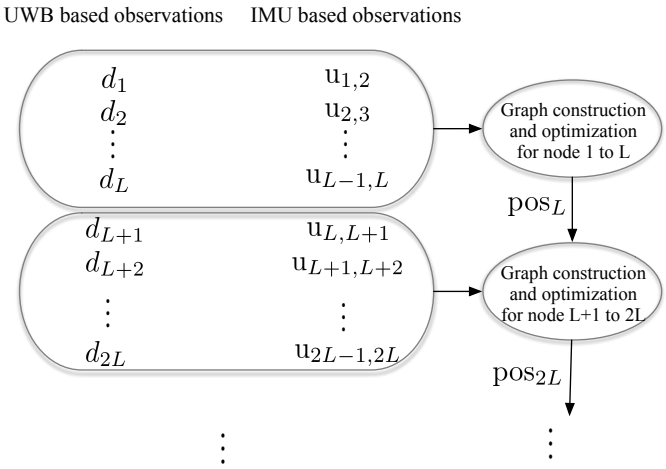

Fig. 3. The graph is broken down to enable on-line processing.

As Fig. 2 shows, the obstruction of human body can add up to an extra ranging error of about 1.3 m.

Therefore, this should be taken account into consideration in forming the UWB based edges. Here we form a simple error between the k_{th} node and the UWB anchor q in 6,

$$\mathbf{e}_{\text{UWB}}(k,q) = \begin{cases} a(d_k - dist(k,q)), & (d_k - dist(k,q)) > 0 \\ d_k - dist(k,q), & (d_k - dist(k,q)) < 0 \end{cases} \tag{6}$$

where a is a coefficient with value $0 < a < 1$, the coefficient is added because we want to make the situations where the ranging measurement is less than the ground truth to contribute more to the error function. Herein we use the value $a = 0.5$. The function $dist(k,q)$ denotes the distance between the estimated $\mathbf{pos}_k$ and the position of the UWB anchor q, and d_k is the corresponding range measurement. Then the error function of this edge contributing to the overall error function is

$$f_{\text{UWB}}(k,q) = \Omega_{\text{UWB}} \mathbf{e}^2_{\text{UWB}}(k,q) \tag{7}$$

The information matrix Ω_{UWB} in this case is a scale value, which corresponds to the reciprocal of the variance of the UWB based range measurements. In our implementation the value is set to be 1.

B. The overall graph

1) The overall error function: As aforementioned, the graph construction process is in essence forming the overall error function to be minimized in the graph optimization process. The error function reveals the extent how the measurements are in consistence with the state estimates. In our implementation, the overall function is the sum of errors derived from the IMU based edges and the UWB based edges, which is

$$f_{\text{overall}}(.) = \sum_{k=2}^{N} f_{\text{IMU}}(k-1,k) + \sum_{k=1}^{N}\sum_{q=1}^{M} f_{\text{UWB}}(k,q) \tag{8}$$

where the number N is the number of nodes and M is the number of UWB anchors. If there is no range measurement between a pose and a UWB anchor, the $f_{\text{UWB}}(.)$ is set to be 0. This can make the Jacobian matrix of the error function to be sparse, which is favorable in terms of computational cost for graph optimization.

2) Considerations for online processing: Although the estimation accuracy and robustness is enhanced by adopting all past observation, the computational cost can grow with time. This can lead to too many nodes and edges and the optimization can be too slow. To overcome this, we propose to break down the large graph to render possible online processing. As Fig. 3 shows, the observations before the L^{th} step is firstly adopted to generate the graph and then do the optimization for trajectory initialization and calibration. Then the estimated $\mathbf{pos}_L$ is used as the initial pose for the next graph processing cycle, which adopts the observations from the $L+1^{th}$ step to the $2L^{th}$ step. The first two graph processing cycles is equivalent to break down one large graph with $2L$ nodes to two graphs with L nodes each. In this way, the large graph with too many nodes which is hard to optimize is avoided and online processing is possible. The breaking down of graphs is continued for later observations to come.

IV. Experiment

One simulation and two real scenario tests are designed to verify the proposed method. For easy implementation, we always assume that the IMU based trajectories starts at position (0,0). As for the heading, we assume that the initial heading of the IMU module is 0. However, as the way the IMU mounted on the foot differs and the pedestrian may not take the first step at the IMU's heading, the actual initial headings of the IMU based trajectories in the tests are seemed random. Also, the trajectories are designed to overlap with each other for a few iterations, where the consistency of trajectories can be easily observed. For the real scenario tests, the IMU module we used is from [15], which can be regarded as a black box and can generate step-wise (one position output per step) position

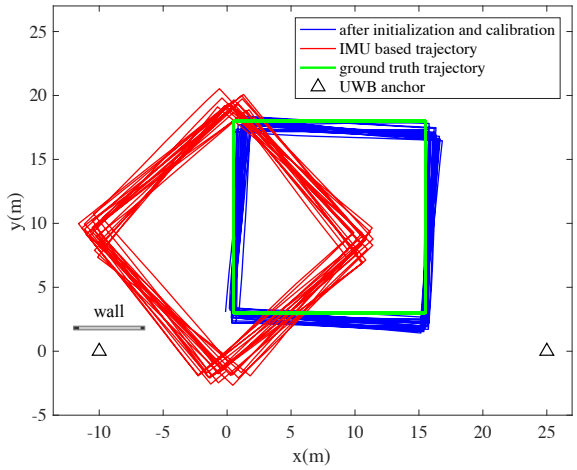

Fig. 4. The trajectories in simulation

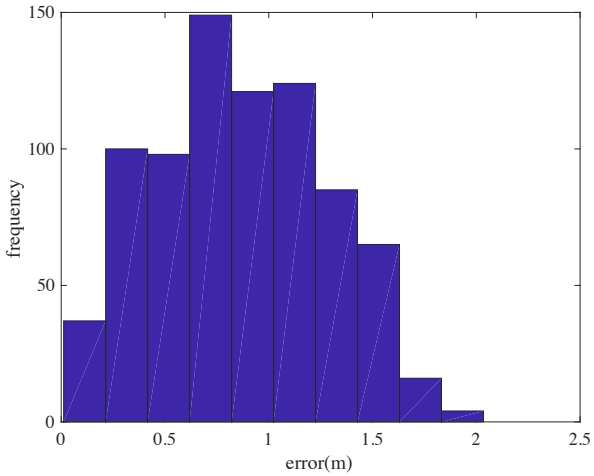

Fig. 5. The histogram of position errors after initialization and calibration

updates. The UWB ranging module is from [16], which has low power consumption and easy to carry. Both the output of the IMU module and the UWB module are transferred to a phone through Bluetooth connection, where the data are synchronized for later processing.

A. Simulation

A trajectory of 800 steps are generated, the ground truth trajectory has a square shape and is iterated for 20 times. Each step has a stride length of 1.5 m. Some noises are added to the ground truth trajectory to form the IMU based trajectory. We assume both the stride length noise and the heading noise is Gaussian and the variances are sn_{var} and hn_{var} respectively. They are set to 0.05 m^2 and 0.01 rad^2 in our implementation. As shown in Fig. 4, two UWB anchors are set in the scene. A wall is added near the left anchor, we assume that if there is wall between the anchor and the pedestrian, an extra error of 1.5 m is added due to NLoS. Under line of sight (LoS) situations, the ranging error is Gaussian and has a variance of 0.5 m^2. After trajectory initialization and calibration, the resulting trajectory is the blue lines. As can obviously seen from Fig. 4, the resulting trajectory corresponds well with the ground truth trajectory. The initialization error for the position and heading is about 1.2 m and 0.1 rad. The histogram of the position error is shown in Fig. 5.

B. Real scenario tests

Two tests are carried out and the first one is in a basket ball court, where the true trajectory can be marked according to the lines in the court. In Fig. 6, the IMU based trajectories are not overlapped in different iterations due to inertial drifts. After processing with our method, the trajectories are well calibrated and can match the lines of the court. The initialization error in this case is 1.3 m for position and 0.16 rad for heading respectively. Unlike the simulation case, where position errors at each step can be calculated, in this test only the errors at the corners are calculated, which can be easily marked.

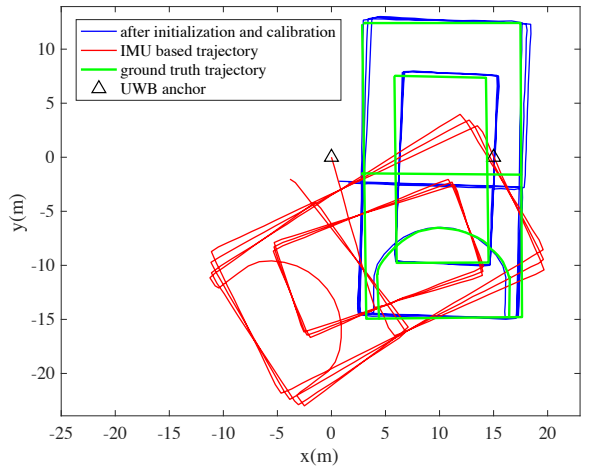

Fig. 6. The trajectories for test 1

This is because in the real scenario case, the steps taken are uneven, the ground truth positions corresponding to each steps are not easily found. The mean position error at these corners is about 1.1 m. The second one is carried out in a normal indoor and outdoor situation, as shown in Fig. 7, the big circle shaped trajectory is when the pedestrian walks to the outside and no ranging measurements are available. Fig. 8 shows the enlarged indoor part of the trajectories. We can see that as the pedestrian walks out and comes back indoor, the error of trajectories becomes very obvious, while using our method can well compensate the errors.

Fig. 9 and Fig. 10 show the distance differences between the UWB range measurements and the distance calculated according to the results of position estimations. These errors can be regarded as residual errors after optimization. As we can see that in both of the figures, the number of samples whose error is larger than 0 is more than those less than 0. This corresponds well with the fact that the range measurements are

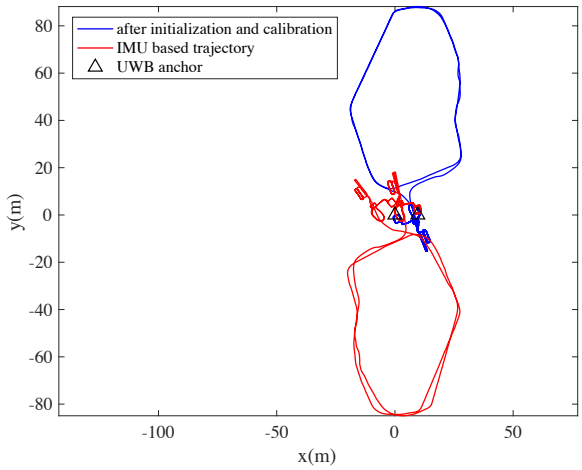

Fig. 7. The trajectories for test 2

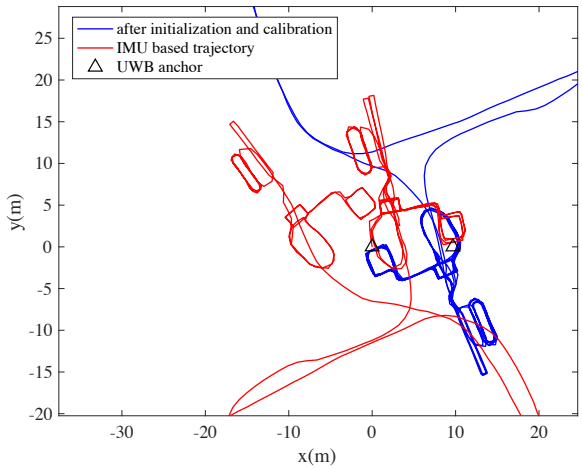

Fig. 8. The enlarged trajectories for test 2

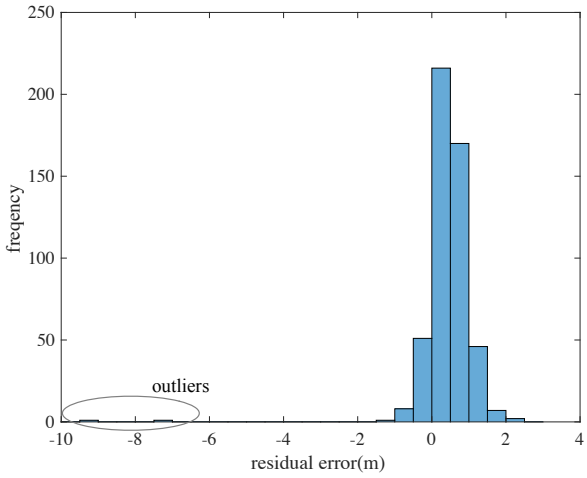

Fig. 9. The residual errors of range measurement in test 1

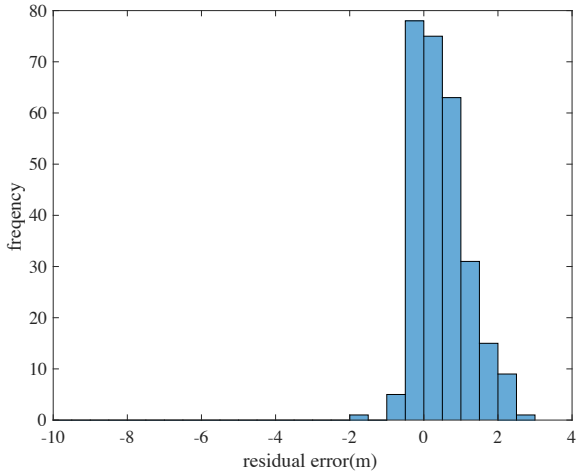

Fig. 10. The residual errors of range measurement in test 2

often over estimated in NLoS situations, e.g. obstructed by the human body. Our method can also cope with the situations with outlier range measurements like that in test one.

C. Comparisons with a PF

For fusion of DR and UWB based range measurements, PFs are often adopted because it can represent the unknown initial states with particles distributed in the state space. The PF is also more robust than Kalman filters because PFs can deal with nonlinear and none Gaussian filtering. In this paper, the proposed method is compared with a PF based method in [11] and the same method with backtrack. Here we use the dataset in test one, where the positioning errors can be calculated at the corners of the courts. The number of particles is set to 1000, which is considered enough in the implementation. As particle filtering is a probabilistic method, the results for each run may be different. We have run the PF based method for 1000 times, the results comparisons in term of mean error, maximum error and processing time are shown in Table.I. [1]

Noting that here the mean and maximum values are with respect to the running times. For our method, as the result is not random, we only run it once, so that the mean error and maximum error for this run is the same. For the PF based method and PF based with backtrack, the errors and the processing time are taken from the mean value of the 1000 runs. Our method outperforms the PF based methods in terms of accuracy and processing time. Though PF with backtrack can further improve the robustness and accuracy compared with PF without backtrack, there are still many reasons deteriorating the accuracy like less particle number, type of processing noise added and so on.

[1]All the methods are run using Matlab on a PC with 2 cores Intel Core i5 processor.

TABLE I
COMPARISONS OF OUR METHOD, PF BASED METHOD AND PF BASED METHOD WITH BACKTRACK

Method	Mean error	Maximum error	Mean Time
Our method	1.1 m	1.1 m	1.56 s
PF	1.7 m	6.2 m	13.76 s
PF with backtrack	1.2 m	3.2 m	33.43 s

V. CONCLUSION

A method for trajectory initialization and trajectory calibration using a foot-mounted IMU and UWB rang anchors is proposed in this paper. The IMU can provide relative DR trajectories and the UWB anchor can provide ranging measurements. A graph SLAM based framework is adopted, where the poses of the pedestrian at different steps are the nodes in the graph, IMU based measurements and the ranging measurements are the edges in the graph. After optimizing the graph using all observations, the positions at different steps are estimated as a batch. Both simulations and the real scenario tests have validated the good performance of the proposed method. At last, the proposed method is compared with the particle filter based methods with and without backtrack. The proposed method is superior to these methods in terms of both robustness and processing time.

REFERENCES

[1] E. Foxlin, "Pedestrian tracking with shoe-mounted inertial sensors," *IEEE Computer Graphics and Applications*, vol. 25, no. 6, pp. 38–46, 2005.

[2] A. R. Jiménez, F. Seco, J. C. Prieto, and J. Guevara, "Indoor pedestrian navigation using an INS/EKF framework for yaw drift reduction and a foot-mounted IMU," in *2010 7th Workshop on Positioning, Navigation and Communication*, 2010, pp. 135–143.

[3] J. O. Nilsson, A. K. Gupta, and P. Handel, "Foot-mounted inertial navigation made easy," in *IPIN 2014 - 2014 International Conference on Indoor Positioning and Indoor Navigation*, 2014, pp. 24–29.

[4] J.-O. Nilsson, I. Skog, and P. Händel, "A note on the limitations of ZUPTs and the implications on sensor error modeling," in *Proceeding of 2012 International Conference on Indoor Positioning and Indoor Navigation (IPIN), 13-15th November 2012*. KTH, ACCESS Linnaeus Centre, 2012.

[5] C. Gentile and A. Kik, "A Comprehensive Evaluation of Indoor Ranging Using Ultra-wideband Technology," *EURASIP J. Wirel. Commun. Netw.*, vol. 2007, no. 1, p. 12, 2007. [Online]. Available: http://dx.doi.org/10.1155/2007/86031

[6] J. J. Leonard, R. J. Rikoski, P. M. Newman, and M. Bosse, "Mapping Partially Observable Features from Multiple Uncertain Vantage Points," *The International Journal of Robotics Research*, vol. 21, no. 10-11, pp. 943–975, 2002.

[7] E. Menegatti, A. Zanella, S. Zilli, F. Zorzi, and E. Pagello, "Range-only SLAM with a mobile robot and a Wireless Sensor Networks," in *2009 IEEE International Conference on Robotics and Automation*, 2009, pp. 8–14.

[8] A. Savioli, E. Goldoni, P. Savazzi, and P. Gamba, "Low complexity indoor localization in wireless sensor networks by UWB and inertial data fusion," *arXiv preprint arXiv:1305.1657*, 2013.

[9] F. Zampella, A. D. Angelis, I. Skog, D. Zachariah, and A. Jiménez, "A constraint approach for UWB and PDR fusion," in *2012 International Conference on Indoor Positioning and Indoor Navigation (IPIN)*, 2012, pp. 1–9.

[10] J.-O. Nilsson, D. Zachariah, I. Skog, and P. Händel, "Cooperative localization by dual foot-mounted inertial sensors and inter-agent ranging," *EURASIP Journal on Advances in Signal Processing*, vol. 2013, no. 1, p. 164, 2013.

[11] Y. Gu, Q. Song, M. Ma, Y. Li, and Z. Zhou, "A unanimous trajectory calibration framework based on anchors in inertial pedestrian positioning," *Sensor Review*, vol. 37, no. 4, pp. 410–418, 2017.

[12] G. Grisetti, R. Kummerle, C. Stachniss, and W. Burgard, "A Tutorial on Graph-Based SLAM," *IEEE Intelligent Transportation Systems Magazine*, vol. 2, no. 4, pp. 31–43, 2010.

[13] M. I. A. Lourakis and A. A. Argyros, "SBA: A Software Package for Generic Sparse Bundle Adjustment," *ACM Trans. Math. Softw.*, vol. 36, no. 1, pp. 1–30, 2009. [Online]. Available: http://doi.acm.org/10.1145/1486525.1486527

[14] R. Kümmerle, G. Grisetti, H. Strasdat, K. Konolige, and W. Burgard, "G2o: A general framework for graph optimization," in *2011 IEEE International Conference on Robotics and Automation*, 2011, pp. 3607–3613.

[15] Q. Song, L. Yanghuan, M. Ming, and Z. Zhimin, "Low-cost miniaturized foot-mounted pedestrian navigation system," in *2013 International Conference on Indoor Positioning and Indoor Navigation (IPIN)*, 2013.

[16] "http://www.decawave.com/products/dw1000." [Online]. Available: http://www.decawave.com/products/dw1000